AN INVESTIGATION OF TRAVELLING WAVE AND DRIFT TUBE IMS SEPARATIONS OF PROTEIN ION CHARGE STATES AND THEIR FRAGMENTS

Steven Pringle[1]; Kevin Giles[1]; Stormy L Koeniger[2]; Stephen Valentine[3]; Robert Bateman[1]; David E Clemmer[2];

[1]Waters MS Technology Center, Floats Road, Wythenshawe, Manchester, UK; [2]Department of Chemistry, Indiana University, Bloomington, IN; [3]Predictive Physiology and Medicine, Bloomington, IN

OVERVIEW

AIM

- To compare two new ion mobility spectrometry techniques; Travelling Wave Ion Mobility and Tandem Drift Tube IMS for the separation of fragment ions from intact proteins according to ion charge states and their cleavage type.

Results

- Similar results were obtained both in terms of spectral decongestion and the ability to extract families of ions corresponding to specific fragment ion types and charge states.

INTRODUCTION

Although extensive work involving the separation and characterization of protein and peptide ions has been carried out, few studies have examined the mobilities of fragment ions. In this study, two new ion mobility spectrometry (IMS) techniques, travelling wave (TWIMS) and a tandem drift tube (TDTIMS) have been used to separate the ubiquitin fragment ions (formed by collision induced dissociation) prior to analysis by MS. In both approaches fragment ions appear to fall into families according to their charge states. The separation significantly reduces spectral congestion associated with the mass spectra, making it possible to observe and identify many fragment ions that would not be observed with MS/MS alone. Overall, the ability to observe and identify these small features improves the fraction of the protein sequence that can be associated with specific fragments. In some cases, mobility separation appears to create families of ions for specific fragment ion types; for example, families of both y-type and b-type ions have been observed.

EXPERIMENTAL

The two instruments used in this study were a tandem drift tube/oa-ToF (TDIMS) instrument shown in figure 1 and a hybrid quadrupole/TWIMS/oa-ToF shown in figure 2.

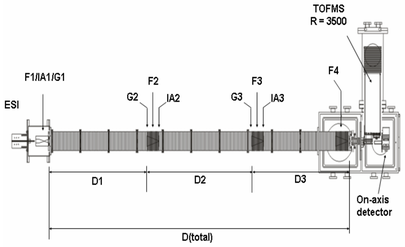

Figure 1 : Schematic diagram of the tandem drift tube/oa-ToF instrument (TDTIMS) used in this study.

The tandem drift tube has been described elsewhere[1]; briefly ions produced by an ESI source are accumulated in an ion funnel (F1), and periodically released into a drift tube (D1). Ions exiting the first drift region enter an ion funnel (F2) containing an ion gate and activation region.(G2&IA2). Following this is a drift region (D2) with an ion funnel/gate/activation assembly on its exit (F3,G3,IA3) which is followed by a final drift region (D3) and ion funnel (F4) prior to analysis by an oa-ToF. Ions are selectively gated by raising or lowering fields in the gate regions at specific delay times controlled by a pulse delay generator. Collisional activation (IA1, IA2, or IA3) is achieved by increasing the voltage between the last two lenses of each ion funnel. The entire drift tube assembly is ~290 cm long, the field in the drift and funnel regions is 9 V cm^{-1} and 11 V cm^{-1} respectively. The RF applied to the funnels ranged from 70 to 100 V_{PP} at 450 to 480 kHz. The pressure in the drift regions was maintained at ~ 4 mbar of He.

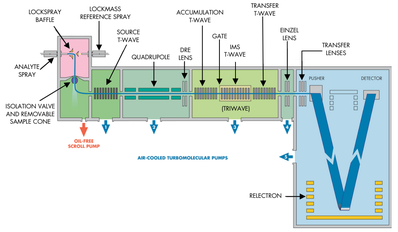

Figure 2 : Schematic diagram of the Waters Synapt HDMS instrument used in this study.

The hybrid quadrupole/TWIMS/oa-ToF used was a Waters Synapt HDMS system; briefly ions produced by an ESI source are sampled by a Z-spray source where they may be activated/fragmented by applying a potential to the sample cone. They pass through a quadrupole that may be set to select a particular m/z. The TWIMS (Triwave) comprises three T-Wave devices[2]. the first device (accumulation T-Wave) accumulates ions and releases them in a short pulse (100µs) every 20 ms into the next device (IMS T-Wave) in which the mobility separation is performed, the final device (transfer T-Wave) is used to transport the separated ions into the oa-ToF for subsequent analysis. Ions may be fragmented on entrance to the accumulation T-Wave and/or the transfer T-Wave. The pressure in the accumulation and transfer T-Wave regions was ~ 10^{-2} mbar of Ar and the pressure in the IMS T-Wave was 0.5 mbar of N_2. The T-Wave pulse velocity and voltage were optimised to provide adequate ion mobility separation.

Ubiquitin (Sigma, 90% purity) was diluted to ~10^{-5} M in a 49:49:2 (% volume) solution of water:acetonitrile:acetic acid. In the case of the data from the tandem drift tube instrument, ions were produced using a pulled capillary tip (75 mm id 360 mm od), at a flow rate of 0.25 µL min^{-1}.

A PEEK microtee was used to couple the capillary tip, the syringe, and a platinum electrode. The pulled capillary was held at a DC bias 2 kV above the drift voltage. In the case of the TWIMS based instrument the Ubiquitin was introduced to the instrument using a standard Waters nano-spray source at a rate of 1µL min^{-1}.

RESULTS

Ubiquitin is a small, 76 amino acid protein that has been studied extensively. Its size, combined with its being a well-characterized system, make ubiquitin a model protein to examine. Figure 3(a) shows an IMS-MS distribution of ubiquitin obtained using the tandem drift tube instrument, a similar IMS-MS distribution obtained using the TWIMS system is shown in figure 4(a).

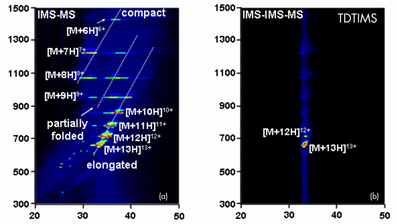

Figure 3 : (a) Drift time vs. m/z plot of ubiquitin ions and (b) $[M+13H]^{13+}$ ion isolated by mobility selection of ions centered at ~33.86 ms with a 50 µs wide pulse at G2. (TDTIMS)

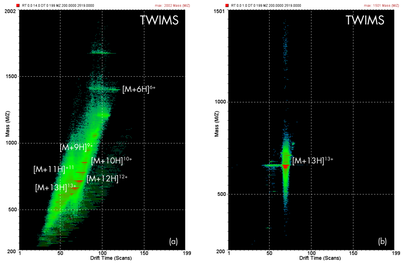

Figure 4 : (a) Drift time vs. m/z plot of ubiquitin ions and (b) $[M+13H]^{13+}$ ion isolated by selection of $[M+13H]^{13+}$ions using the quadrupole (Each drift time scan corresponds to 65 µs). (TWIMS)

Both drift time plots show a range of charge states ($[M+6H]^{6+}$ to $[M+13H]^{13+}$), the tandem drift tube instrument also shows a range of conformations, however, it is only at the lower charge states ($[M+6H]^{6+}$) that multiple drift time peaks are observed using the TWIMS instrument.

Figure 3(b) shows a window of ions selected at G2 having a total drift time of 33.86 ms corresponding to $[M+13H]^{13+}$ ions and figure 4(b) shows a similar plot obtained by selecting the $[M+13H]^{13+}$ ion using the quadrupole ($[M+13H]^{13+}$ total drift time is 4.55 ms). Comparison of the two plots highlights the additional selectivity associated with the tandem IMS approach and its higher drift time resolution.

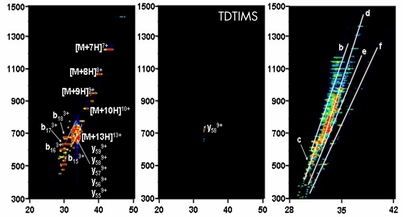

Figure 5 : (a) Drift time vs. m/z plot of mobility-dispersed fragment ions obtained by selection of the $[M+13H]^{13+}$ ion at G2 and activation at IA2, (b) Selection of the y_{58}^{9+} fragment ion at G3 and (c) Fragment ions produced upon activation of the selected y_{58}^{9+} in IA3 then separated based on their mobilities through D3. (TDTIMS)

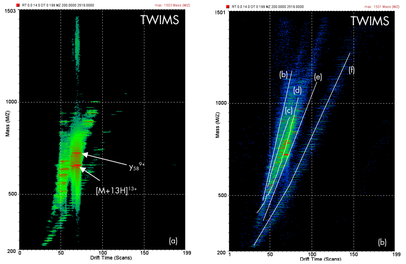

Figure 6 : Drift time vs. m/z plot of mobility-dispersed fragment ions obtained by (a) isolation using the quadrupole and fragmentation of the $[M+13H]^{13+}$ ion on entrance to the accumulation T-Wave, (b) Cone voltage fragmentation of the $[M+13H]^{13+}$ and isolation of the y_{58}^{9+} fragment ion using the quadrupole followed by fragmentation on entrance to the accumulation T-Wave. (TWIMS)

Figures 5(a) and 6(a) show the drift time distribution of ions that are obtained upon activation of the $[M+13H]^{13+}$. This generates a range of new species as well as a series of fragment ions. Again both the TDTIMS and TWIMS instrument give similar results.

Both instruments allow the easy identification of two fragment series : the b_{14}^{3+} to b_{18}^{3+} ions; and, a series of y_{55}^{9+} to y_{59}^{9+} ions. Figure 5(b) and (c) show the selection and subsequent fragmentation of the y_{58}^{9+} ion using the tandem drift cell apparatus. Figure 6(b) shows a similar experiment whereby the y_{58}^{9+} ion is produced in the source using cone voltage fragmentation, it is then selected using the quadrupole and fragmented on entrance to the accumulation T-Wave. In both instruments the resulting fragments are mobility separated.

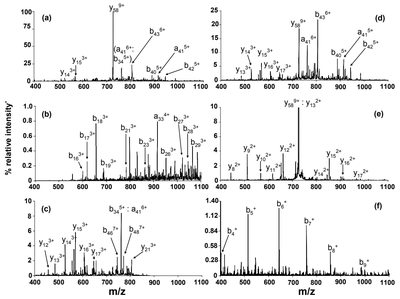

Figure 7: Mass spectra resulting from fragmentation of the y_{58}^{9+} fragment ion produced from the $[M+13H]^{13+}$ of ubiquitin. (a) Total ion mass spectrum obtained by integrating m/z values across the entire drift dimension, (b) through (f) correspond to mass spectra extracted from the specific regions shown in Figure 5(c). (TDTIMS)

The resulting fragment ions fall into families according to similarities in m/z to drift time ratios. The lines that are shown in Figures 5(c) and 6(b) illustrate five regions that are shown as mass spectral slices in Figures 7 and 8. These data illustrate a number of advantages. In the TDTIMS instrument the y_{58}^{9+} precursor dominates the total integrated mass spectrum, however in the TWIMS instrument the y_{13}^{2+} ion is dominant due to a difference in the degree of fragmentation of the y_{58}^{9+} ion. Figure 7(a) and 8(a) shows the total ion spectrum obtained by integrating over the whole drift time dimension. While it is possible to observe and assign several a, b, and y fragments in the total ion mass spectrum, many features become more apparent when the IMS dimension is included. For example, Figures 7(b) and 8(b) show a relatively low-intensity series of high-mobility fragments that includes a set of peaks that can be assigned to most of the b_{16}^{3+} to b_{29}^{3+} series. The mass spectra corresponding to the most intense fragments in the drift time vs. m/z plot are shown in Figure 7 (both c and d). These "slices" contain a series of y^{3+} ions as well as some species that are attributed to higher charge states. Figure 7(e) illustrates a region of the data that is associated with primarily y^{2+} ions which has been assigned to the y_8^{2+} to y_{17}^{2+} series.

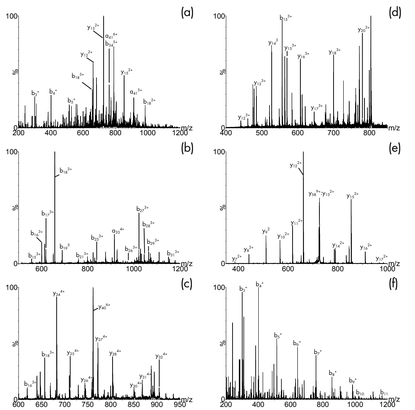

Figure 8: Mass spectra resulting from fragmentation of the y_{58}^{9+} fragment ion produced from the $[M+13H]^{13+}$ of ubiquitin. (a) Total ion mass spectrum obtained by integrating m/z values across the entire drift dimension, (b) through (f) correspond to mass spectra extracted from the specific regions shown in Figure 6(b). (TWIMS)

Figure 8(c) shows a series of fragments that includes a set of peaks that can be assigned to most of the y_{24}^{4+} to y_{32}^{4+} series, whilst figure 8(d) includes a set of peaks that can be assigned to most of the y_{12}^{3+} to y_{20}^{3+} series and figure 8(e) includes a set of peaks that can be assigned to most of the y_7^{2+} to y_{17}^{2+} series. The distributions shown in Figures 7(f) and 8(f) correspond to ions at lower m/z to drift time ratios and include a set of peaks that can be assigned to the b_3^{+} to b_{11}^{+} series.

CONCLUSIONS

The mobility resolution of the (TDTIMS) is greater than that of the TWIMS in the Synapt HDMS system. However the quadrupole mass filter in the latter has greater specificity than IMS. Consequently the two systems provide comparable results both in terms of spectral decongestion and the ability to extract families of ions corresponding to specific fragment ion types and charge states from intact proteins.

REFERENCES

[1] S. I. Merenbloom, S. L. Koeniger, S. J. Valentine, M. D. Plasencia and D. E. Clemmer. *Analytical Chemistry*, 78/8: 2802-2809.

[2] Applications of a travelling wave-based radio frequency only stacked ring ion guide. K.Giles, S.Pringle, K.Worthington, D.Little, J.Wildgoose, R.Bateman. *Rapid Commun. Mass Spectrom. 2004; 18: 2401-2414 The travelling wave device described here is similar to that described by Kirchner in US Patent 5,206,506 (1993).*

720001850EN